journal

J. Am. Ceram. Soc., **84** [12] 2955–61 (2001)

Analyses of Multiple Film Cracking in Film/Substrate Systems

Chun-Hway Hsueh*

Metals and Ceramics Division, Oak Ridge National Laboratory, Oak Ridge, Tennessee 37831

Multiple film cracking in a film/substrate system is analyzed in the present study. The system is subjected to residual stresses before loading. A constant displacement rate is applied unidirectionally to stretch the system. An analytical model is developed to derive the stress distribution in the system, and the film-cracking problem is analyzed using both the strength and the energy criteria. The predicted crack spacing as a function of the applied strain is compared with experimental measurements of multiple cracking of SiO_x films with various thicknesses on poly(ethylene terephthalate) substrates. Comparison is also made between the present and other predictions.

I. Introduction

CRACKING of brittle films on substrates is a major reliability problem in electronic devices, protective coatings, and other film applications.[1] Because of the processing and the mismatch in the thermomechanical properties between films and substrates, as-fabricated film/substrate systems are generally subjected to residual stresses. These residual stresses combined with external stresses applied on the system can lead to cracking and/or delamination of the film. Such damage inevitably degrades the performance and reliability of the system. Hence, the mechanical integrity and the adhesion of the film become a major concern, and various efforts have been devoted to analyzing residual stresses and film cracking/delamination in film/substrate systems.[1–6] The technique of multiple film cracking has been developed to characterize the film strength in which the system is pulled uniaxially in the plane of the film.[7–12] As the system is stretched, cracks transverse to the loading direction develop in the brittle film. The number of cracks increases as the applied strain is increased, and the relation between the measured mean crack spacing and the applied strain has been used to characterize the film strength or fracture energy.

To analyze the multiple film cracking problem, the shear lag model has been adopted which was originally developed by Cox[13] to analyze the stress transfer between the fiber and the matrix and was subsequently extended to analyze multiple fiber fracture in a unidirectional fiber-reinforced composite.[14,15] Based on the concept of the shear lag model for a cylindrical geometry, the stress transfer between the film and the substrate in a planar geometry has been analyzed.[4,8,10,16] It is noted that the stress transfer is dictated by the shear stress at the film/substrate interface. Depending upon the properties of the interface, two types of the shear lag model have been developed. The first one considers that the substrate is ductile and the interface yields such that the interfacial shear stress is governed by a constant yield strength of the substrate.[4,8] In this case, the stress distribution in the system can be readily related to the yield strength. The second one considers the interface to be elastic and remaining bonded. In this case, the interfacial shear stress is often assumed to be proportional to the relative displacement between film and substrate, and a fitting parameter hence exists in the stress transfer solutions.[8,10,16] This fitting parameter can be determined by fitting theoretical results to experimental data.

It is noted that the multiple film cracking problem has also been analyzed elsewhere[17,18] using the energy release rate solution in Tada *et al.*'s handbook[19] for the problem of a periodic set of parallel edge cracks propagating perpendicular to the free surface of a semi-infinite plane. However, in this case, the film and the substrate are assumed to have the same elastic properties.

The purpose of the present study is to develop a rigorous analytical model for the elastic stress transfer between a film and a substrate and to analyze the multiple film-cracking problem. First, an analytical model is developed to derive a closed-form solution to predict the stress distribution in the film. Then, both the strength and the energy criteria are adopted to predict film cracking, and the predicted relation between the mean crack spacing and the applied strain is compared to the experimental measurements. Finally, the present analytical solution derived from the shear lag model is compared to the solution derived from the energy release rate in Tada *et al.*'s handbook.[17–19]

II. Analytical Modeling

The film/substrate system is shown in Fig. 1, in which the Cartesian coordinates, x and y, are used. The film is bonded to the substrate at $x = a$, and the free surfaces of the substrate and the film located respectively at $x = 0$ and $x = b$, such that the thicknesses of the substrate and the film are respectively a and $b - a$. The film is subjected to a mismatch strain, ε_m, relative to the substrate before loading. A uniform strain, ε_l, is loaded on the system in the y-direction. The film is cracked with a uniform crack spacing, $2l$, and a periodic array of film segments is formed. In this case, only one film segment is required in the analyses, and the y-coordinate is selected such that the ends of the selected film segment are located at $y = \pm l$ (Fig. 1).

(1) Stress Distribution

The equilibrium equation between the normal stress in the loading direction, σ_y, and the shear stress, τ_{xy} $(=\tau)$, is[20]

$$\frac{\partial \sigma_y}{\partial y} + \frac{\partial \tau}{\partial x} = 0 \tag{1}$$

Integration of Eq. (1) over the thickness of the film and then division by its thickness yield

$$\frac{\partial}{\partial y}\left[\left(\frac{1}{b-a}\right)\int_a^b \sigma_y \, dx\right] + \frac{1}{b-a}\int_a^b \frac{\partial \tau}{\partial x} dx = 0 \tag{2}$$

Since the film is relatively thin, the stress variation through the thickness can be ignored. Letting σ_f represent the average value of

A. G. Evans—contributing editor

Manuscript No. 188187. Received October 26, 2000; approved August 9, 2001.
This research was sponsored by the U.S. Department of Energy, Division of Materials Sciences and Engineering, Office of Basic Energy Sciences, under Contract No. DE-AC05-000R22725 with UT-Battelle.

*Member, American Ceramic Society.

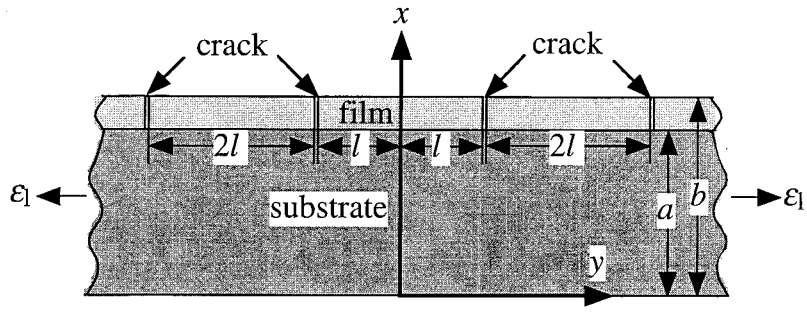

Fig. 1. Schematic showing multiple film cracking with a uniform crack spacing, $2l$, in a film/substrate system subjected to residual stresses and a loading strain, ε_1.

σ_y over the film thickness and using the free surface condition that $\tau = 0$ at $x = b$, Eq. (2) becomes

$$\frac{d\sigma_f}{dy} = \frac{\tau_i}{b - a} \tag{3}$$

where τ_1 is the shear stress at the interface (i.e., at $x = a$).

An approximation is taken for the substrate in satisfying the equilibrium equation, such that Eq. (1) is satisfied in an average (with respect to the x-direction) sense.[†] In this case, the x-dependence of σ_y is ignored in the equilibrium equation, and the gradient of σ_y in the y-direction in the substrate can be approximated by a function of y, i.e.,

$$\frac{\partial\sigma_s}{\partial y} = f(y) \tag{4}$$

where $\sigma_s = \sigma_y$ for the substrate. The approximate x-dependence of σ_s can be obtained by solving the approximate equilibrium equation which is shown as follows.

Continuity of the shear stress at the interface (i.e., $\tau = \tau_1$ at $x = a$) is required. Solution of Eqs. (1) and (4) subjected to the continuity condition and the free surface condition (i.e., $\tau = 0$ at $x = 0$) yields

$$\tau = \frac{x\tau_i}{a} \qquad (\text{for } 0 \le x \le a) \tag{5}$$

With $\sigma_x = 0$ and the displacement in the x-direction being negligible, τ can be related to the displacement in the y-direction, w, by

$$\tau = \left(\frac{E_s}{2(1 + \nu_s)}\right)\left(\frac{dw}{dx}\right) \tag{6}$$

where E_s and ν_s are Young's modulus and Poisson's ratio of the substrate, respectively. Combination of Eqs. (5) and (6) and integration yield

$$\tau_i = \frac{E_s(w_a - w_0)}{a(1 + \nu_s)} \tag{7}$$

$$\tau = \frac{xE_s(w_a - w_0)}{a^2(1 + \nu_s)} \tag{8}$$

[†]The same approximation has been adopted in analyzing the two-dimensional stress transfer problem for a plate embedded in a matrix, and the predicted stress distribution in the system agrees well with the finite element result.[21]

where $w = w_0$ at $x = 0$, and $w = w_a$ at $x = a$. The displacement, w, can be derived from Eqs. (6) and (8), such that

$$w = w_0 + \frac{x^2}{a^2}(w_a - w_0) \tag{9}$$

Differentiation of Eq. (9) with respect to y and then multiplication by E_s give

$$\sigma_s = \sigma_{s0} + \frac{x^2}{a^2}(\sigma_{sa} - \sigma_{s0}) \tag{10}$$

where $\sigma_s = \sigma_{s0}$ at $x = 0$, and $\sigma_s = \sigma_{sa}$ at $x = a$. The approximate x-dependence of σ_s in the substrate is described by Eq. (10).

The mechanical equilibrium condition between the applied strain ε_1 and the stress distribution in the system requires that

$$\int_0^a \sigma_s\, dx + (b - a)\sigma_f = [aE_s + (b - a)E_f]\varepsilon_1 \tag{11}$$

Substitution of Eq. (10) into Eq. (11) gives

$$\sigma_{s0} = -\frac{\sigma_{sa}}{2} - \frac{3(b - a)\sigma_f}{2a} + \frac{3}{2}\left[E_s + \frac{(b - a)E_f}{a}\right]\varepsilon_1 \tag{12}$$

where E_f is Young's modulus of the film. Combining Eqs. (3), (7), and (12) and differentiation with respect to y yield

$$\frac{d^2\sigma_f}{dy^2} = \frac{3}{2a(b - a)(1 + \nu_s)}\left\{\sigma_{sa} + \frac{(b - a)\sigma_f}{a} - \left[E_s + \frac{(b - a)E_f}{a}\right]\varepsilon_1\right\} \tag{13}$$

The solution of σ_f from Eq. (13) is subjected to the following three boundary conditions: The film is bonded to the substrate at the interface, the film is stress-free at the ends, and the system is symmetric with respect to $y = 0$; i.e.,

$$\frac{\sigma_{sa}}{E_s} = \frac{\sigma_f}{E_f} + \varepsilon_m \qquad (\text{at } x = a) \tag{14a}$$

$$\sigma_f = 0 \qquad (\text{at } y = l) \tag{14b}$$

$$\tau = 0 \qquad (\text{at } y = 0) \tag{14c}$$

With the above three boundary conditions, the solution is

$$\sigma_f = E_f\left[\varepsilon_1 - \frac{\varepsilon_m}{1 + \dfrac{(b - a)E_f}{aE_s}}\right]\left[1 - \frac{\cosh(\alpha y)}{\cosh(\alpha l)}\right] \tag{15}$$

$$(\text{for } -l \le y \le l)$$

where

$$\alpha = \left[\frac{3}{2a(b-a)(1+\nu_s)}\left(\frac{E_s}{E_f}+\frac{b-a}{a}\right)\right]^{1/2} \tag{16}$$

The stress distribution along the film segment is described by Eq. (15).

(2) Strength Criterion for Film Cracking

The maximum stress within the film occurs at the center of the film segment (i.e., at $y = 0$), such that

$$\sigma_f^{max} = E_f\left[\varepsilon_l - \frac{\varepsilon_m}{1+\dfrac{(b-a)E_f}{aE_s}}\right][1-\text{sech}\,(\alpha l)] \tag{17}$$

Cracking of the film segment would occur at $y = 0$ when σ_f^{max} reaches the film strength, σ_{str}. The critical applied strain, ε_c, for film cracking to initiate can be obtained from Eq. (17). When an uncracked film (i.e., $l \gg 0$ in Eq. (17)) is subjected to ε_c, the corresponding σ_f^{max} reaches σ_{str}, such that

$$\sigma_{str} = E_f\left[\varepsilon_c - \frac{\varepsilon_m}{1+\dfrac{(b-a)E_f}{aE_s}}\right] \tag{18}$$

The relation between the loading strain, ε_l, and the film segment with a length $2l$ to break into two equal-length segments can be obtained from Eq. (17) by substituting σ_f^{max} with σ_{str} (Eq. (18)) such that

$$\varepsilon_l = \frac{\cosh\,(\alpha l)\varepsilon_c - \dfrac{\varepsilon_m}{1+\dfrac{(b-a)E_f}{aE_s}}}{\cosh\,(\alpha l) - 1} \tag{19a}$$

or

$$l = \frac{1}{\alpha}\cosh^{-1}\left[\frac{\varepsilon_l - \dfrac{\varepsilon_m}{1+\dfrac{(b-a)E_f}{aE_s}}}{\varepsilon_l - \varepsilon_c}\right] \tag{19b}$$

It is noted that the result of Eq. (19) is based on the condition of a constant film strength during the film segmentation process.

(3) Energy Criterion for Film Cracking

For the problem considered in the present study, the following energy terms are involved: (1) the elastic strain energy in the film and the substrate, (2) the fracture energy of the film, and (3) the work done by loading. Since the geometry considered in the present study is two-dimensional, the energy terms considered are per unit depth in the direction normal to the xy plane. For the geometry defined in Fig. 1, the stress in the film segment with length $2l$ is described by Eq. (15) before film cracking occurs. The elastic strain energy in the film, U_{f1}, is

$$U_{f1} = \left(\frac{b-a}{2E_f}\right)\int_{-l}^{l}\sigma_f^2\,dy \tag{20}$$

When cracking occurs at $y = 0$, two film segments of equal length, l, are formed. Redefining the coordinate position of $y = 0$ at the center of each film segment, the stress distribution in each film segment can be obtained from Eq. (15) by substituting l with $l/2$. The elastic strain energy in these two film segments, U_{f2}, is

$$U_{f2} = \frac{b-a}{E_f}\int_{-l/2}^{l/2}\left\{E_f\left[\varepsilon_l - \frac{\varepsilon_m}{1+\dfrac{(b-a)E_f}{aE_s}}\right]\times\left[1-\frac{\cosh\,(\alpha y)}{\cosh\,(\alpha l/2)}\right]\right\}^2 dy \tag{21}$$

The elastic energy change in the film due to cracking, ΔU_f, is

$$\Delta U_f = U_{f2} - U_{f1} \tag{22}$$

Compared to ΔU_f, the change in elastic strain energy in the substrate is negligible because the substrate is much thicker than the film, no cracking occurs in the substrate, and the substrate is subjected to a constant strain, ε_l. The energy required for film cracking, ΔG_f, is

$$\Delta G_f = 2(b-a)\Gamma \tag{23}$$

where Γ is the film fracture energy. Since film cracking occurs at a fixed loading strain, ε_l, there is no change of work due to film cracking. Hence, the energy balance equation for film cracking becomes

$$\Delta U_f + \Delta G_f = 0 \tag{24}$$

Solution of Eqs. (20) to (24) yields

$$\begin{aligned}\Gamma = \frac{E_f}{2\alpha}&\left[\varepsilon_l - \frac{\varepsilon_m}{1+\dfrac{(b-a)E_f}{aE_s}}\right]^2\\ &\times\left\{4\left[\frac{\exp(\alpha l/2)-\exp(-\alpha l/2)}{\exp(\alpha l/2)+\exp(-\alpha l/2)}\right]\right.\\ &-\frac{\exp(\alpha l)-\exp(-\alpha l)+2\alpha l}{\exp(\alpha l)+\exp(-\alpha l)+2}\\ &-2\left[\frac{\exp(\alpha l)-\exp(-\alpha l)}{\exp(\alpha l)+\exp(-\alpha l)}\right]\\ &\left.+\frac{1}{2}\left[\frac{\exp(2\alpha l)-\exp(-2\alpha l)+4\alpha l}{\exp(2\alpha l)+\exp(-2\alpha l)+2}\right]\right\}\end{aligned} \tag{25}$$

The critical applied strain, ε_c, for film cracking to initiate can be obtained from the solution of ε_l in Eq. (25) by letting $l \to \infty$, such that the relation between Γ and ε_c is

$$\Gamma = \frac{3E_f}{4\alpha}\left[\varepsilon_c - \frac{\varepsilon_m}{1+\dfrac{(b-a)E_f}{aE_s}}\right]^2 \tag{26}$$

Combination of Eqs. (25) and (26) yields

$$\varepsilon_l = \frac{\varepsilon_c - \dfrac{(1-\beta)\varepsilon_m}{1+\dfrac{(b-a)E_f}{aE_s}}}{\beta} \tag{27a}$$

where β is a function of αl given by

$$\begin{aligned}\beta = \sqrt{\frac{2}{3}}&\left\{4\left[\frac{\exp(\alpha l/2)-\exp(-\alpha l/2)}{\exp(\alpha l/2)+\exp(-\alpha l/2)}\right]\right.\\ &-\frac{\exp(\alpha l)-\exp(-\alpha l)+2\alpha l}{\exp(\alpha l)+\exp(-\alpha l)+2}\\ &-2\left[\frac{\exp(\alpha l)-\exp(-\alpha l)}{\exp(\alpha l)+\exp(-\alpha l)}\right]\\ &\left.+\frac{1}{2}\left[\frac{\exp(2\alpha l)-\exp(-2\alpha l)+4\alpha l}{\exp(2\alpha l)+\exp(-2\alpha l)+2}\right]\right\}^{1/2}\end{aligned} \tag{27b}$$

Hence, assuming a constant film fracture energy, Γ, the relation between the loading strain, ε_l, and the film segment with a length $2l$ to break into two equal-length segments is described by Eq. (27).

III. Results

Experiments of multiple film cracking have been performed in several studies.[7–12] The mismatch strain in the film is usually ignored; nevertheless, it has been measured by Yanaka *et al.*[10] The experimental measurements by Yanaka *et al.* are hence chosen for comparison with present predictions. First, experimental measurements by Yanaka *et al.* are summarized. Second, the strength and the fracture energy of the film are derived based on the measured critical applied strain in initiating film cracking. Third, the predicted stress distribution in the film is shown. Fourth, the predicted crack spacing versus applied strain relation is compared with measurements. Finally, the present prediction is compared to the prediction derived from Tada *et al.*'s handbook of stress analysis of cracks.

(1) Summary of Yanaka's Experiment[10]

The multiple film cracking tests were performed on SiO_x films with various thicknesses (75, 123, 215, and 660 nm) deposited on 12 μm thick poly(ethylene terephthalate) (PET) substrates. The initial slopes of the stress–strain curves of the bare substrate and the substrate with film were used to obtain Young's moduli of the substrate and the film/substrate system, respectively. These two Young's moduli were then used to derive Young's modulus of the film, E_f. It is noted that the derived E_f were scattered for the different film thicknesses, and an average value was adopted. The elastic constants of the system thus measured were $E_f = 43$ GPa, $E_s = 4.7$ GPa, $\nu_s = 0.44$, and the yield strain of the PET substrate was ~2.2%. The film was deposited by vacuum evaporation and was subjected to residual compression after cooling to room temperature. The mismatch strain in the film relative to the substrate, ε_m, was calculated from the measured curvature and the estimated elastic constants of the system and is listed in Table I. A constant displacement rate was applied unidirectionally to stretch the system. The critical applied strain, ε_c, to initiate film cracking for each film thickness is also listed in Table I, and the mean crack spacing, $\bar{l}$, was measured during the test. It is noted that the measured crack spacing had a statistical distribution around the mean value, $\bar{l}$. At a given applied strain, the longest segments would break into halves with more or less half lengths, while shorter segments would remain unbroken. Hence, the longest and the shortest crack spacings would be $2l$ and l, respectively, when the loading strain is ε_l. The average crack spacing, $\bar{l}$, was approximated as the average of the longest and the shortest crack spacings, such that

$$\bar{l} = \frac{3l}{2} \tag{28}$$

(2) Film Strength and Fracture Energy

Using the data of the mismatch strain, ε_m, and the crack initiation strain, ε_c, in Table I as well as the elastic constants listed in Section III(1), the strength and the fracture energy for initial film cracking can be calculated from Eqs. (18) and (26), respectively, and the results are shown in Fig. 2. The film strength, σ_{str}, decreases initially with increasing film thickness and then becomes insensitive to film thickness when the film thickness is greater than 200 nm. The fracture energy of the film, Γ, decreases initially and then increases as the film thickness increases. Not knowing the accuracy of the data (e.g., the mismatch strain and Young's moduli) adopted in calculating σ_{str} and Γ, it is premature to discuss the variations of σ_{str} and Γ with the film thickness. However, using a fracture toughness $K_c = 0.79$ MPa · m$^{1/2}$ (Ref. 9) for the glass film, the corresponding fracture energy, $\Gamma = K_c^2/2E_f$, becomes ~7 J/m^2, which is in the range of Γ predicted in Fig. 2. Also, if both the strength criterion and the energy criterion predict the same crack initiation strain, ε_c, the relation between σ_{str} and Γ can be obtained by equating ε_c in Eqs. (18) and (26), such that

$$\sigma_{str} = \sqrt{\frac{4\alpha E_f \Gamma}{3}} \tag{29}$$

Since the relation between σ_{str} and Γ involves α, which is a function of the dimension and elastic constants of the system (see Eq. (16)), the strength and the fracture energy cannot both be the intrinsic properties of the film. It has been argued that the thin film influences the stress field in the substrate only within a certain boundary zone in the neighborhood of the film. Outside the boundary zone, the stress field in the substrate is not perturbed by the presence of the film. Hence, an effective substrate thickness instead of the actual substrate thickness should be used in analytical modeling.[22] This effective substrate thickness scales with the film thickness,[22] and the scaling parameter should be a function of the Young's modulus ratio of film to substrate. Assuming a be proportional to $b - a$ in Eq. (16), the film strength becomes inversely proportional to the square root of the film thickness when the fracture energy is a constant (see Eq. (29)).

(3) Stress Distribution in Film Segment

Two data sets with large (155 μm) and small (4.56 μm) crack spacings for the 123 nm thick film from Yanaka's measurements are adopted in the present study to predict the stress distribution in the film segment to elucidate the essential trends. The critical loading strain for initial film cracking, ε_c, is 1.2%, and the corresponding mean crack spacing, $\bar{l}$, is 155 μm (i.e., $l = 103.3$ μm). When the loading strain, ε_l, is increased to 3.35%, the corresponding $\bar{l}$ is 4.56 μm (i.e., $l = 3.04$ μm). Using Eq. (15) and $\varepsilon_m = 0.63\%$ (Table I), the predicted stress distributions in the film segment are shown in Figs. 3(a) and (b), respectively, for $l = 103.3$ and 3.04 μm at different applied strains. The stress distribution in the film segment, $-l \le y \le l$, is symmetric with respect to the

Table I. Data of the Mismatch Strain (ε_m) in the SiO_x Film Relative to the PET Substrate and of the Critical Applied Strain (ε_c) for Initial Film Cracking[10]

$b - a$ (nm)†	ε_m (%)	ε_c (%)
73	1.01	1.84
123	0.63	1.2
215	0.48	0.94
660	0.24	0.69

†SiO_x film thickness.

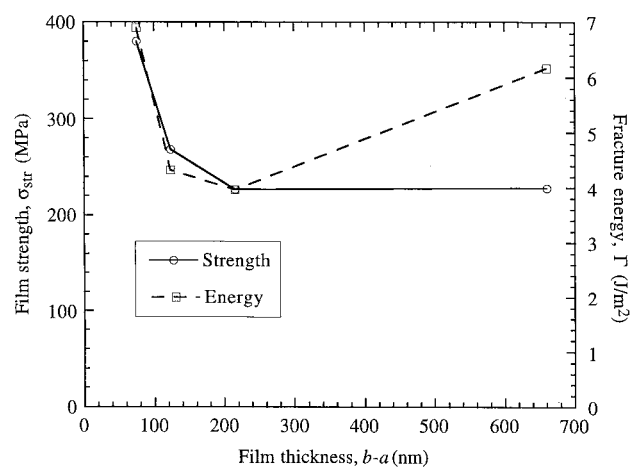

Fig. 2. Calculated film strength, σ_{str}, and fracture energy, Γ, for the SiO_x film/PET substrate system based on the measured critical loading strain in initiating film cracking.

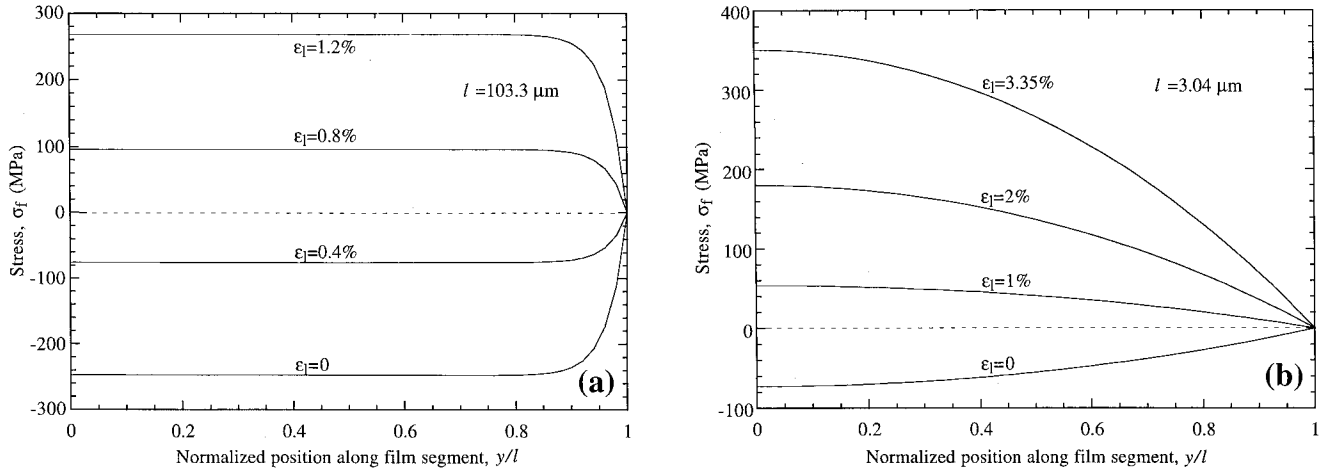

Fig. 3. Predicted stress distribution, σ_f, along (a) a long film segment with half length $l = 103.3$ μm, and (b) a short film segment with half length $l = 3.04$ μm at different loading strains, ε_l, for a 123 nm thick SiO_x film on a PET substrate.

center of the film (i.e., $y = 0$), and the stress distribution in half of the film segment, $0 \leq y \leq l$, is shown in Fig. 3.

The stress is zero at the end of the film segment (i.e., at the crack), and its magnitude increases with the distance from the crack and reaches an asymptotic value when the film segment is sufficiently long (e.g., see Fig. 3(a)). In the absence of the loading strain, the residual stress in the film is compressive. The stress in the film, σ_f, becomes tensile when the tensile loading strain is sufficiently large. Based on the strength criterion, film cracking occurs when σ_f reaches the strength, σ_{str}. For a long film segment (Fig. 3(a)), the region having the plateau value of σ_f extends from the center of the film segment to a great distance which, in turn, results in a great area of potential locations for film cracking. Conversely, for a short film segment (Fig. 3(b)), the region with highest σ_f concentrates at the center of the film segment and the potential location for film cracking is limited to the area of the film center. Hence, when film segmentation initially occurs, the lengths of the film segments have a great variation. The lengths of the film segments become more uniform in the later stage of film segmentation. This phenomenon is in agreement with the experimental observation.[23]

(4) Mean Crack Spacing

Using Eqs. (19) and (27), the predicted mean crack spacing, $\bar{l}$ (see Eq. (28)), versus loading strain, ε_l, based on the strength and the energy criteria are shown in Figs. 4(a), (b), (c), and (d), respectively, for 75, 123, 215, and 660 nm thick films. It is noted that limitations exist in the present analyses which are discussed as follows.

First, the analysis is two-dimensional, and the dimension normal to the *xy* plane in Fig. 1 is not considered. If the system has a large dimension normal to the *xy* plane, care should be taken in including this dimension in the analysis. While the plain strain condition can be used when the system is subjected to only loading in the *y*-direction, it cannot be used in the presence of residual stresses. For example, in the absence of cracking, a biaxial-residual stress (i.e., the stress normal to the *xy* plane equals that in the *y*-direction) exists in the system. However, a three-dimensional analytical model is out of the scope of the present study. Also, evaluation of the mismatch strain from the curvature was based on a two-dimensional case.[10] Hence, the present two-dimensional analysis is used to compare with the measurements, in which data were derived based on a two-dimensional consideration.

Second, linear elasticity is considered in the present analytical modeling. While the yield strain of the PET substrate is ~2.2%,[10] it was reported by Leterrier *et al*. that the permanent strain of the SiO_x/PET system upon unloading is negligible for an applied strain up to 4%.[23] Hence, plasticity of the substrate can be ignored for loading strains up to 4%. In the presence of substrate plasticity, the load on the system is lower than that described by Eq. (11) for an applied strain ε_l, and the film should be subjected to a stress lower than that described by Eq. (15) which, in turn, results in a greater crack spacing than that predicted in Fig. 4. However, both the measurements and the predictions in Fig. 4 show that $\bar{l}$ decreases as ε_l increases and the decreasing rate becomes smaller as ε_l increases. When ε_l is greater than ~4%, the decreasing rate is relatively small (i.e., the curve is relatively smooth). Including plasticity in the analysis, the decreasing rate will become even smaller. Hence, plasticity is expected not to play a significant role in the predicted $\bar{l}$ vs ε_l curve for the strain range considered in the present study.

Third, a constant strength or fracture energy of the film is considered in relating ε_l to $\bar{l}$ in the present analysis (see Eqs. (19) and (27)). The film strength, σ_{str}, or fracture energy, Γ, is derived from the critical strain, ε_c, in initiating film cracking. When a Weibull distribution of σ_{str} (or Γ) is considered, cracking should start from a lower value of σ_{str}, and σ_{str} increases progressively during the multiple cracking process. In this case, the predicted $\bar{l}$ at a fixed ε_l should be greater than that based on a constant σ_{str} approach.

Despite the limitations of the present analysis discussed above, fair agreement is obtained for the mean crack spacing versus loading strain relation between the prediction and the measurement (Figs. 4(a) to (d)). Compared to the strength criterion, the energy criterion predicts a greater mean crack spacing for fixed film thickness and loading strain. It is noted that for high loading strains (>~4%), the predicted mean crack spacing increases with the film thickness. Whereas the measurement shows the same trend, the rate of increasing is greater in the measurement, such that the predicted curves are above the experimental data for 75 nm film thickness (Fig. 4(a)) and below the experimental data for 660 nm film thickness (Fig. 4(d)). The reason for this discrepancy is presently unknown and is subjected to further research.

(5) Comparison with Prediction Derived from Tada et al.'s Handbook

Considering a periodic set of parallel edge cracks subjected to an opening stress in a semi-infinite plane, the energy release rate for cracks propagating perpendicular to the free surface can be found in Tada *et al*.'s handbook in a graphic form, which is then fitted by a polynomial.[19] Based on this information, the change in strain energy to create a set of cracks of depth equal to the film thickness, $b - a$, is derived.[17,18] Then, by minimizing the total energy of the cracked film (i.e., the strain energy in the cracked

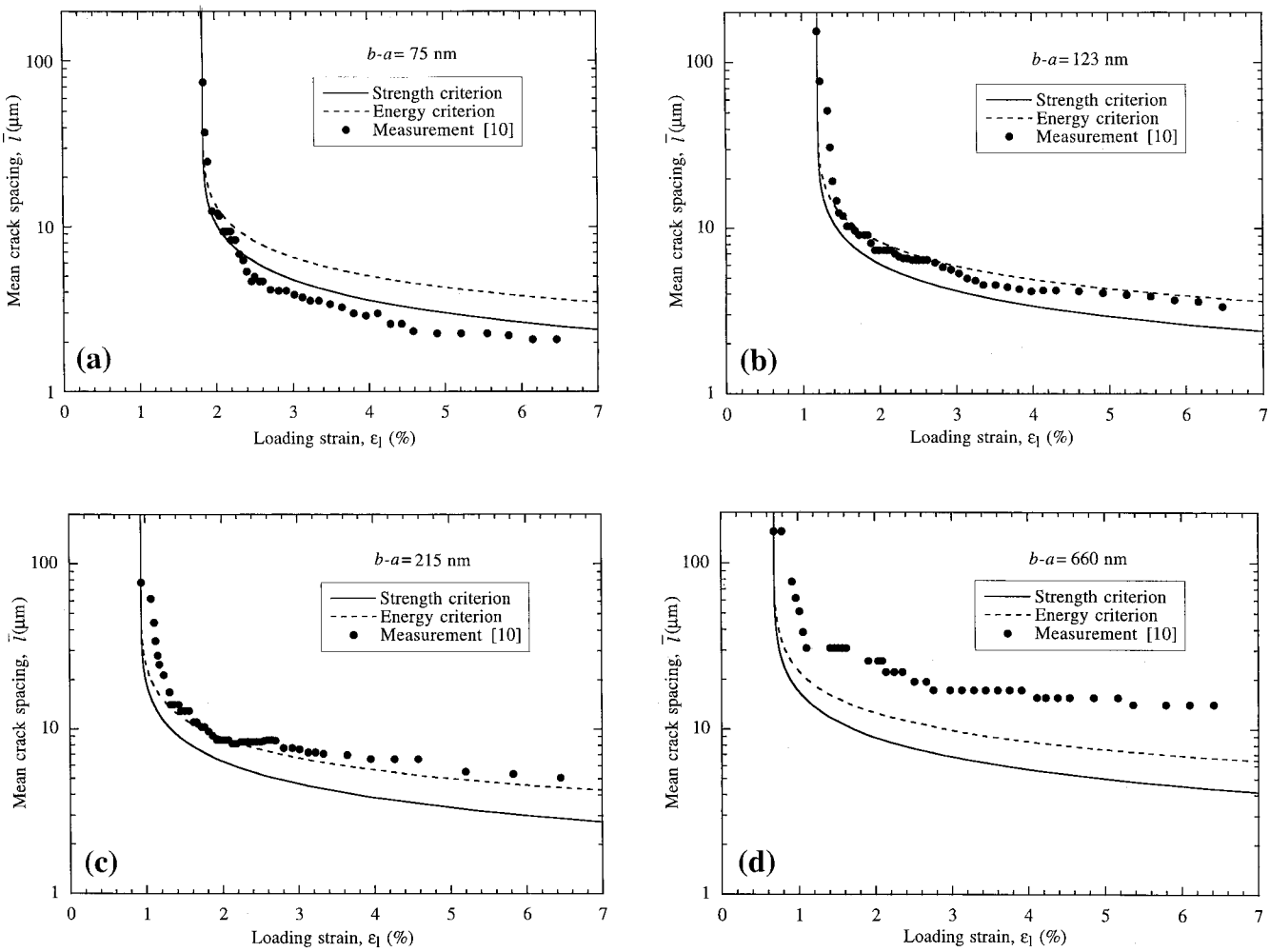

Fig. 4. The predicted and the measured mean crack spacings, $\bar{l}$, as functions of the loading strain, ε_l, for film thicknesses, $b - a$, of (a) 75, (b) 123, (c) 215, and (d) 660 nm in SiO_x/PET systems.

film and the fracture energy of the film), the relation between the equilibrium crack spacing, l, and the applied strain, ε, is obtained, such that[17]

$$\frac{l}{b-a} \approx 5.6 \sqrt{\frac{\Gamma}{E\varepsilon^2(b-a)}} \qquad (\text{for } E\varepsilon^2(b-a)/\Gamma \geq 0.5) \tag{30}$$

It is noted that the above approximation is limited to the case that the film and the substrate have the same elastic properties.

The prediction of Eq. (25) in the present study is compared to the above prediction (Eq. (30)). To achieve this, the mismatch strain, ε_m, is ignored, the film and the substrate are assumed to have the same elastic properties, and ν_s is set to be 0 (in order to eliminate the difference between plane stress and plane strain solutions) in using Eq. (25). However, the effective substrate thickness[22] is required in order to complete the calculation. Assuming the effective substrate thickness be 10, 20, or 40 times of the film thickness, the predictions from Eq. (25) are shown in Fig. 5. The prediction from Thouless *et al.*'s analysis (Eq. (30)) is also shown. While Eq. (30) is an approximate solution, both Eqs. (25) and (30) show similar predictions in Fig. 5.

IV. Concluding Remarks

An analytical model is developed to derive closed-form analytical solutions in the present study to analyze the elastic stress transfer problem in the film/substrate system. Residual stresses are included in the analysis. Both the strength and the energy criteria are adopted to predict film cracking when the system is subjected to a unidirectional tensile strain. The present model is applied to multiple film cracking of the SiO_x film/poly(ethylene terephthalate) (PET) substrate system. While the present analysis is limited

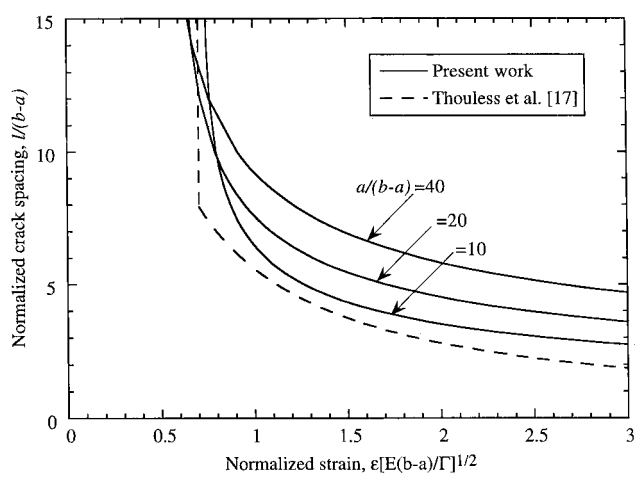

Fig. 5. Normalized crack spacing, $l/(b - a)$, as a function of the normalized strain, $\varepsilon[E(b - a)/\Gamma]^{1/2}$, showing the comparison between the present prediction and Thouless *et al.*'s prediction.

to a two-dimensional elastic case and a Weibull distribution of the film strength (or fracture energy) is not considered, the experimental measurement is subjected to errors in determining the residual strain and Young's modulus of the thin film. With no fitting parameters in the present analytical model, the predicted results rely on the accuracy of the input material properties. The agreement in the mean crack spacing versus loading strain relation between the prediction and the measurement is fair (Figs. 4(a) to (d)). The agreement between the present prediction (Eq. (25)) and the prediction of Eq. (30) using Tada *et al*.'s solution is also fair (Fig. 5). However, to fully characterize the film strength (or fracture energy) of the film and to judge whether the strength or the energy criterion is superior in analyzing the film cracking problem, improvement of the model by considering three-dimensional elastic-plastic analysis is required and it will be developed in the future.

Acknowledgments

I am grateful to Dr. M. Yanaka for making the detailed data from his recent paper[10] available, and I thank Dr. P. F. Becher, Prof. G. M. Pharr, and Dr. M. J. Lance for reviewing the manuscript.

References

[1]W. D. Nix, "Mechanical Properties of Thin Films," *Metall. Trans.*, **20A**, 2217–45 (1989).

[2]A. G. Evans and J. W. Hutchinson, "The Thermomechanical Integrity of Thin Films and Multilayers," *Acta Metall. Mater.*, **43** [7] 2507–30 (1995).

[3]C. H. Hsueh and A. G. Evans, "Residual Stresses in Metal/Ceramic Bonded Strips," *J. Am. Ceram. Soc.*, **68** [5] 241–48 (1985).

[4]M. S. Hu and A. G. Evans, "The Cracking and Decohesion of Thin Films on Ductile Substrates," *Acta Metall.*, **37** [3] 917–25 (1989).

[5]T. R. Watkins and D. J. Green, "Fracture Behavior of Chemically-Vapor-Deposited SiC-Coated Graphite: I, Experimental Results," *J. Am. Ceram. Soc.*, **76** [12] 3066–72 (1993).

[6]D. J. Green, "Crack Arrest and Multiple Cracking in Glass through the Use of Designed Residual Stress Profiles," *Science*, **283**, 1295–97 (1999).

[7]D. C. Agrawal and R. Raj, "Measurement of the Ultimate Shear Strength of a Metal–Ceramic Interface," *Acta Metall. Mater.*, **37** [4] 1265–70 (1989).

[8]F. S. Shieu, R. Raj, and S. L. Sass, "Control of the Mechanical Properties of Metal–Ceramic Interfaces Through Interfacial Reactions," *Acta Metall. Mater.*, **38** [11] 2215–24 (1990).

[9]Y. Leterrier, J. Andersons, Y. Pitton, and J.-A. E. Månson, "Adhesion of Silicon Oxide Layers on Poly(ethylene terephthalate). II: Effect of Coating Thickness on Adhesion and Cohesive Strengths," *J. Polym. Sci. B: Polym. Phys.*, **35**, 1463–72 (1997).

[10]M. Yanaka, Y. Tsukahara, N. Nakaso, and N. Takeda, "Cracking Phenomena of Brittle Films in Nanostructure Composites Analysed by a Modified Shear Lag Model with Residual Strain," *J. Mater. Sci.*, **33**, 2111–19 (1998).

[11]H. Bordet, M. Ignat, and M. Dupeux, "Analysis of the Mechanical Response of Film on Substrate Systems Presenting Rough Interfaces," *Thin Solid Films*, **315**, 207–13 (1998).

[12]B. F. Chen, J. Hwang, G. P. Yu, and J. H. Huang, "*In Situ* Observation of the Cracking Behavior of TiN Coating on 304 Stainless Steel Subjected to Tensile Strain," *Thin Solid Films*, **352**, 173–78 (1999).

[13]H. L. Cox, "The Elasticity and Strength of Paper and Other Fibrous Materials," *Br. J. Appl. Phys.*, **3**, 72–79 (1952).

[14]A. Kelly and W. R. Tyson, "Tensile Properties of Fibre-Reinforced Metals: Copper/Tungsten and Copper/Molybdenum," *J. Mech. Phys. Solids*, **13**, 329–50 (1965).

[15]J. K. Kim, L. M. Zhou, and Y. W. Mai, "Stress Transfer in the Fibre Fragmentation Test," *J. Mater. Sci.*, **28**, 6233–45 (1993).

[16]N. Laws and G. J. Dvorak, "Progressive Transverse Cracking in Composite Laminates," *J. Compos. Mater.*, **22**, 901–16 (1988).

[17]M. D. Thouless, E. Olsson, and A. Gupta, "Cracking of Brittle Films on Elastic Substrates," *Acta Metall. Mater.*, **40** [6] 1287–92 (1992).

[18]J. W. Hutchinson and Z. Suo, "Mixed Mode Cracking in Layered Materials," *Adv. Appl. Mech.*, **29**, 63–191 (1992).

[19]H. Tada, P. C. Paris, and G. R. Irwin, "The Stress Analysis of Cracks Handbook," Paris Production, Inc., St. Louis, MO, 1985, p. 15.1.

[20]S. P. Timoshenko and J. N. Goodier, *Theory of Elasticity*; p. 97. McGraw-Hill, New York, 1951.

[21]C. H. Hsueh, E. R. Fuller Jr., S. A. Langer, and W. C. Carter, "Analytical and Numerical Analyses for Two-Dimensional Stress Transfer," *Mater. Sci. Eng.*, **A268** [1–2] 1–7 (1999).

[22]G. P. Cherepanov, "On the Theory of Thermal Stresses in a Thin Film on a Ceramic Substrate," *J. Appl. Phys.*, **75**, 844–49 (1994).

[23]Y. Leterrier, L. Boogh, J. Andersons, and J.-A. E. Månson, "Adhesion of Silicon Oxide Layers on Poly (ethylene terephthalate). I: Effect of Substrate Properties on Coating Fragmentation Process," *J. Polym. Sci. B: Polym. Phys.*, **35**, 1449–61 (1997). □